



## QUANTITATIVE ASSESSMENT OF RIVER ICE GENERATION USING SHORE-BASED PHOTOGRAMMETRIC TECHNIQUES

Ansari, Saber<sup>1,3</sup>, Rennie, Colin D.<sup>1</sup>, Seidou, Ousmane<sup>1</sup>, Malenchak, Jarrod<sup>2</sup>, and Ghareh Aghaji Zare, Soheil<sup>1</sup>

<sup>1</sup> Department of Civil Engineering, University of Ottawa, Canada, K1N 6N5

<sup>2</sup> Section Head, Ice, and Environmental Engineering, Department of Water Resources Engineering, Manitoba Hydro, Winnipeg, Canada

<sup>3</sup> [sansa048@uottawa.ca](mailto:sansa048@uottawa.ca)

**Abstract:** Ice cover has great influence on hydraulics and morphology of rivers in high latitude areas of the northern hemisphere. Ice generation rate dictates the ice cover behavior and propagation during the river freeze-up. However our understanding of the process is limited, due to insufficient observation data sets. The collection of reliable hydraulic data under the ice cover conditions is difficult, dangerous, or even impossible using traditional methods. In this study, a time series of images captured by a digital time-lapse camera was used to estimate the ice generation rate at two locations along the Lower Nelson River (LNR), an open water patch and on a border ice leading edge. It was observed that ice periodically formed and was advected out of the persistent open water patch. The image time series were geo-rectified and then ice generation in the patch was estimated based on observed changes in ice volume. The volume of thermal ice generation in the open water patch and on the shores of an island was estimated using the automated image analysis algorithm. Application of this algorithm in similar studies and acquiring more comprehensive data will lead us to more precise equations for estimation of river ice production.

### 1 Introduction:

Ice-covered lakes and rivers influence living conditions in countries of colder regions. Canadian lakes and rivers are exposed to extreme cold weather that promotes river ice cover formation in most areas. Although ice cover may be beneficial for the economy of the region, such as the recreational industry, it also may lead to various adverse effects such as loss of marine navigation, ice jamming floods and frost heaving damage to hydraulic structures. River flow characteristics are influenced by the presence of river ice in the whole process of pre-formation, formation and deterioration. Several researchers have studied the influence of river ice cover on river hydraulics, morphology and sediment transport such as Ghareh Aghaji Zare, et al. (2016a) and Guo et al. (2016). Moreover, ice cover phenomena can also influence water quality and mixing ability (Ranjie & Huimin 1987; P.A. Chambers, et. al. 1993; Tang et al., 2016). Despite these previous studies, still much remains to be understood. Studying river ice cover processes in field locations is expensive and can be dangerous. Therefore scientists are interested in monitoring techniques in which a vast set of data is acquirable with less effort and resources.

In many research studies of different fields, photogrammetry has been introduced as an art and technology of data acquisition. Oblique terrestrial imagery however has been employed as an easy to

use, efficient and economic method of monitoring and data gathering in earth sciences. Several studies have used terrestrial photogrammetry for data acquisition in various fields, such as glaciology, land cover investigations, watershed management, transportation, river engineering and sediment transport studies. Monitoring of river ice processes both in lakes and rivers, and both remote and shore-based imagery have been used for different purposes such as navigation and ice jam related floods (Jędrzychowski & Kujawski 2014).

### 1.1 Research area:

For an improved understanding of the river ice processes, a comprehensive research investigation has been conducted since 2012 on Nelson River, Manitoba, Canada. The Nelson River is one of the largest rivers across North America, with a length of 2575 km and a drainage area of about 892300 km<sup>2</sup>. This large river has great importance for the economy of the region considering its tremendous potential in hydropower generation and fisheries. Nelson River drains Lake Winnipeg to Hudson's Bay through several lakes such as Sipiwesk, Split and Stevens. The study reach is on the Lower Nelson River, LNR, a regulated semi-alluvial river. This research was conducted between Limestone Generation Station (LGS) and Gillam Island, the last 102 km of the river (Figure1).

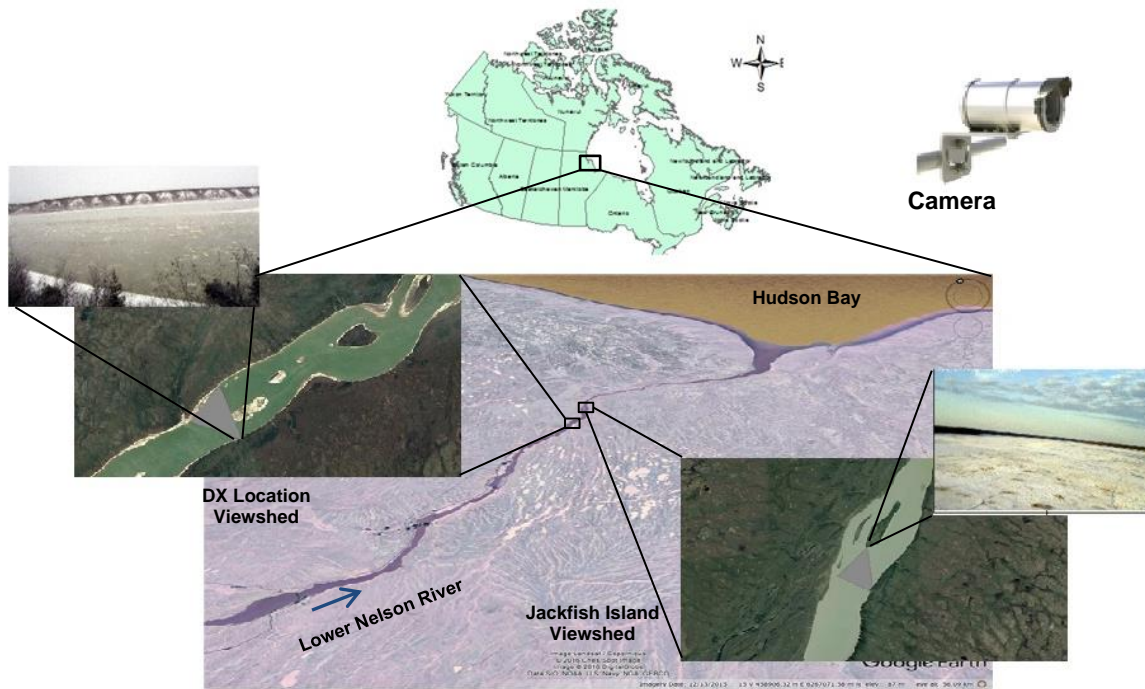


Figure 1: Study area locations and mounted camera along LNR; DX, and Jackfish Island (respectively, 65 km and 50 km upstream of Gillam Island)

### 1.2 Methodology:

This study included long-term hydraulic data gathering and shore-based monitoring of the river ice processes, during four consecutive winters. A set of bottom mounted instruments including a 1200-kHz Teledyne RD Instrument Acoustic Doppler Current Profiler (ADCP) and a 546-kHz Shallow Water Ice Profiling Sonar (SWIPS), was employed for hydraulic data acquisition of the river. Moreover, two shore mounted high resolution cameras were also used for monitoring purposes. The monitoring system was used for validation of the bottom mounted measurements and to obtain spatial and temporal distribution of the river ice cover. The upward looking ADCP and SWIPS instruments provided comprehensive data

sets of the river ice cover thickness along with water elevation and river flow velocity. On the other hand, to extract quantified data from the time-series images taken at two study sites along the LNR an automated image processing algorithm was also developed (Ansari et al., in revision).

The robust image analysis technique is able to extract and quantify spatial and temporal distribution of the river ice cover. Extracted results of this algorithm can be used for quantification of important ice cover characteristics. The image processing algorithm developed in MATLAB consists of five distinct steps: 1) Preprocessing; in this step initial processing of the images was performed to read date, time, and temperature data recorded on each image. 2) Image registration; this step was developed to rectify the discrepancies caused by camera movements. 3) Image rectification; a currently existing method (Corripio et al. 2004; Härer et al. 2013) was modified for georectification of the oblique images. 4) Target detection; a modified version of the edge sensitive variational image thresholding technique (Ray & Saha 2006) was used to detect ice cover in its different types. 5) Calculations; this step was developed to calculate river ice cover spatial and temporal information.

A brief description of the developed method along with its quantified results to study border ice and thermal ice growth are addressed herein. Application of this method in shore-based monitoring of river ice cover studies will help better understanding of the phenomenon and the continuous advancement of river ice models.

## **2 Apparatus and data:**

Continuous data recording was performed at two locations along the LNR, "DX" and "Jackfish Island" (Figure 1). A Teledyne RD Instruments 1200 kHz Sentinel Acoustic Doppler Current Profiler (ADCP) along with an ASL 546 kHz Multi-Functional Acoustic water column profiler (MF-AWCP) were bottom-mounted at both locations (Ghareh Aghaji Zare et al. 2014). Shore-based monitoring was performed using two Campbell Scientific digital cameras. The CC5MPX weighs about 1.06 kg, with a built-in clock and thermometer. The optical zoom lens of the camera is (4 to 12 mm) and the field of view of the camera is 27° to 80°. The cameras were programmed to take images with the quality of 1280×720 pixels and with a time lapse of every 30 or 60 minutes. Field measurements of the Jackfish Island site performed for three winters starting at December 2012 (~ 6200 images), whereas the DX site measurements were performed for winter 2012 (~ 2300 images). Figure 1 shows two sample pictures taken at the two study locations. The number of the acquired images indicates the importance of developing an automated image analysis algorithm.

## **3 Automated image analysis algorithm:**

An automated image analysis algorithm was developed to extract data from the time series of shore-based images. This algorithm consists of five distinct subroutines as explained here.

### **3.1 Preprocessing:**

The preprocessing step deals with three different tasks prior to proceeding with the main body of the image analysis algorithm. These steps include 1) saving recorded data on each image such as: date, time and temperature. 2) Quality screening of the pictures to eliminate the poor quality images from being processed. 3) Quality increase of the images, by the application of the Median filter (Ansari et al. in revision).

### 3.2 Image registration:

Due to the installation of the cameras on tree trunks, they were subject to some minor movements induced by wind. An image registration subroutine was added to the algorithm to deal with the errors induced by these movements. In this step, the Canny edge detection method (Canny,1986), as well as Hough transform method (Hough, 1962) were used to detect a matching part in all images. Each image was then transformed to the reference image using the method introduced by Goshtasby (1988).

### 3.3 Image rectification:

To be able to extract quantified information from the images, the image rectification subroutine was developed to assign correct and real world coordinates to the corresponding pixels within the images. There have been numerous efforts to address the image rectification problem in the literature(e.g., Corripio 2004; Bourgault 2008; Härer et al. 2013; Messerli & Grinsted 2015). In this algorithm, an existing method of image rectification developed by Corripio 2004 was employed to perform the rectification step. This method applies the camera's intrinsic and extrinsic characteristics and is independent of the Ground Control Points (GCPs) (Härer et al. 2013). In this method pixels of the camera field of view Digital Elevation Model (DEM) are assigned to the pixels of the images. A similar method has also been used in a study by (Härer et al. 2013) to monitor snow cover patterns. In the present algorithm, this method was modified to account for water surface elevation fluctuations using the water elevation measurements (Ansari et al. in revision).

### 3.4 Target detection:

Prior to the final calculation, river ice cover detection is the most important and challenging step. The main goal of this method is the automatic detection of different kinds of river ice cover. In computer vision, target detection is performed using different image thresholding techniques. In image thresholding techniques the image is segmented into several regions of interest. In the developed algorithm the edge sensitive image thresholding method developed by Ray and Saha (2007) was modified to account for altering intensity of pixels for ice and water at different times of the day (Ansari et al. in revision).

### 3.5 Ice characteristics calculations:

The final step of the algorithm is to draw boundaries around the detected river ice cover floes and margins to calculate the area, thickness, and volume of the detected river ice cover. Once the preprocessing, image registration, rectification and target detection steps are performed successfully, other subroutines can also be added to the main code and in the final calculations to extract quantified desired information. Figure 2 shows the developed pipeline of the image analysis algorithm.

## 4 Results:

### 4.1 Model verification:

The main sources of error in this algorithm are the image *georectification* step and the *ice detection* subroutine. Verification of the results acquired by this method was performed distinctly for rectification and detection steps. Ground Control Points taken on the stable ice cover were used to verify the georectification method. Results show that the average distance Root Mean Square Error (RMSE) of the rectified reference images was less than 30 meters. The *target detection* algorithm was verified by manual detection of the river ice cover. The manually detected boundaries of ice cover were then rectified to obtain the area. Comparison of the results extracted by the algorithm and manual detection method led

to error estimation. The target detection RMSE of the analyzed images using the developed algorithm ranged from 20 to 253 square meters over the entire viewshed of 492408 m<sup>2</sup> at Jackfish Island location.

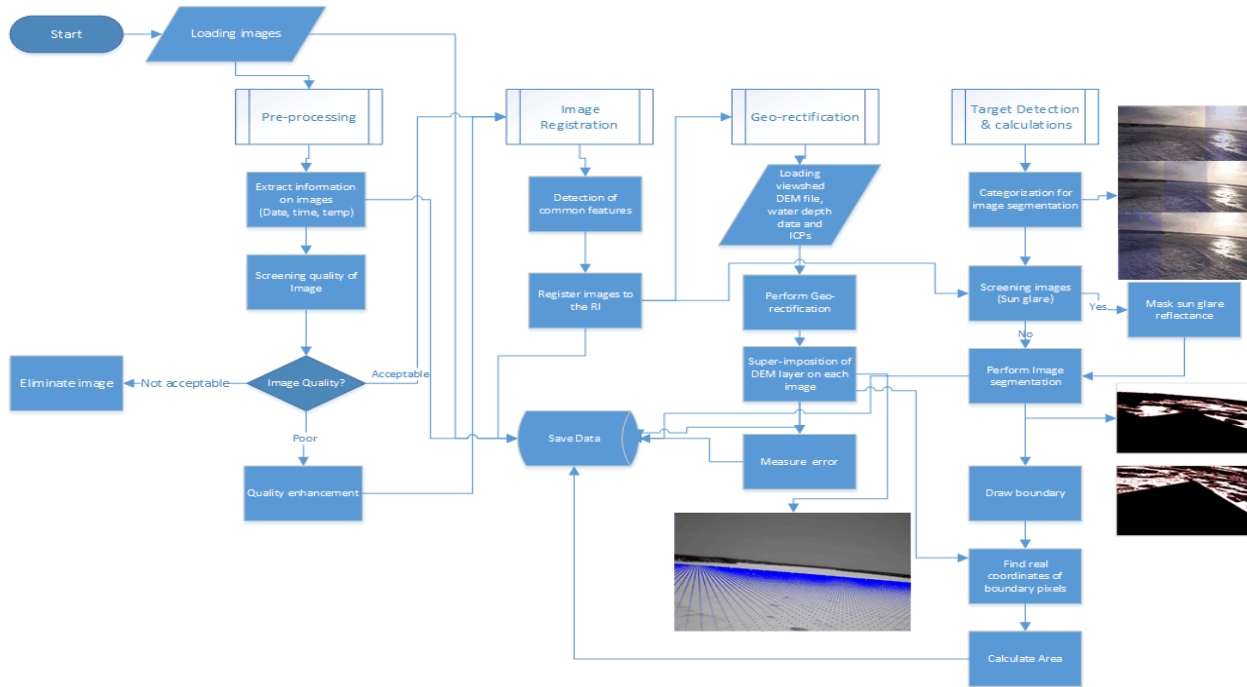


Figure 2: Steps of the developed image analysis pipeline

#### 4.2 Thermal growth of river ice:

One of the major specifications of the locations chosen for field measurements was the occurrence of three main stages of river ice cover processes (freeze-up, consolidation and break-up). Frazil ice generation is the first stage of the freeze-up and river ice cover formation process in LNR. Ice formation occurs in various shapes and types, mainly related to the flow intensity. Border ice and skim ice that form at sections with lower flow intensity are the first types of ice forming in this river. Other than border ice, frazil ice particles that are formed in supercooled water are the primary elements of river ice cover processes. Frazil ice particles adhere to one another growing and forming frazil ice floes. On the other hand frazil particles that are present throughout the cross section of the flow can attach to the objects on the river bottom and form anchor ice. According to the recorded temperature data, air temperature at LNR drops consistently below zero in late October, that is when border ice growth and frazil ice generation initiates.

The analysis of the time series of images taken at two locations of “DX” and “Jackfish Island” presented in (Ansari et al. in revision), led to the investigations over the thermal growth of river ice cover at two locations with different conditions. DX site was located at a steeper section. Flow intensity was higher at this location causing an open area to emerge during the monitoring period. This open water patch was subject to periodical formation of thermal ice. On the other hand, a leading edge of river ice cover detected at the Jackfish Island site was observed to grow gradually starting from mid-January. The thermal growth of river ice cover in the open water patch at DX site and the gradual propagation of river

ice cover leading edge at Jackfish Island site that has been quantified using the automated image analysis algorithm are described in the following sections.

#### 4.3 DX location:

The DX site is located about 35 km downstream of Limestone Generation Station (LGS) and 65 km upstream of Gillam Island. The river at this location has a steeper bed compared to the Jackfish Island site. The high flow intensity at this location forms an area with an open water patch. However, thermal ice formation in the open area periodically covers the open water patch during the winter. Field measurement and monitoring at this location was conducted for one winter (2012-13). Unfortunately, the bottom mount equipment was lost (presumably due to high flow intensity); however, acquired time-series images were used. Observations show that frazil ice generation began as early as mid-October. It was also observed that complete ice cover formed on January 30<sup>th</sup> 2013. Nevertheless, due to high flow intensity, complete cover at this location did not last for long and an open water patch appeared just the day after (Figure 3). The open water area grew with time (see figure 4) until reaching to an equilibrium. Figure 4 shows the growth and shrinkage of the DX open water patch in terms of area percentage of river ice cover. Air temperature and river discharge are also shown in this figure. Flow discharge at the cross section was calculated based on released discharge time shifting at LGS. It was observed that in addition to the frazil ice production at this section that flowed to the downstream; thermal ice periodically formed at the borders of the open area. The thermal growth of river ice on the borders of the open area is the main cause of the calculated open water patch area fluctuations.

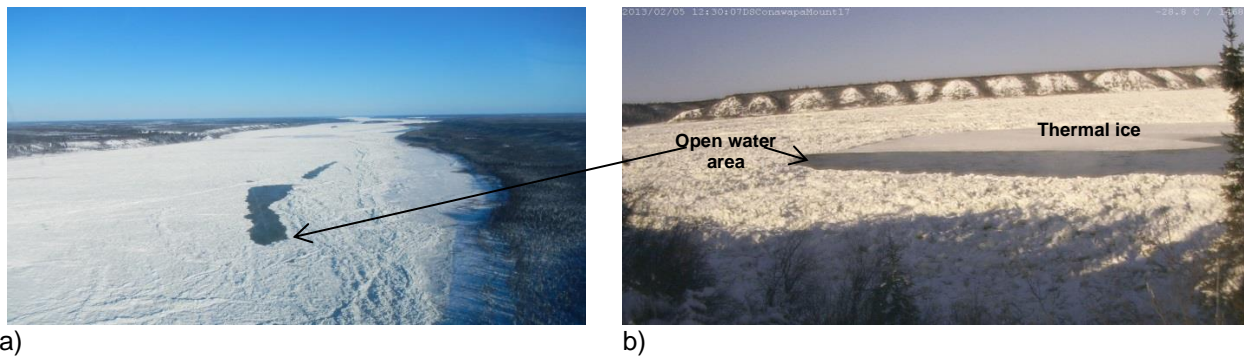


Figure 3: a) Aerial photo, b) shore-based image at DX location

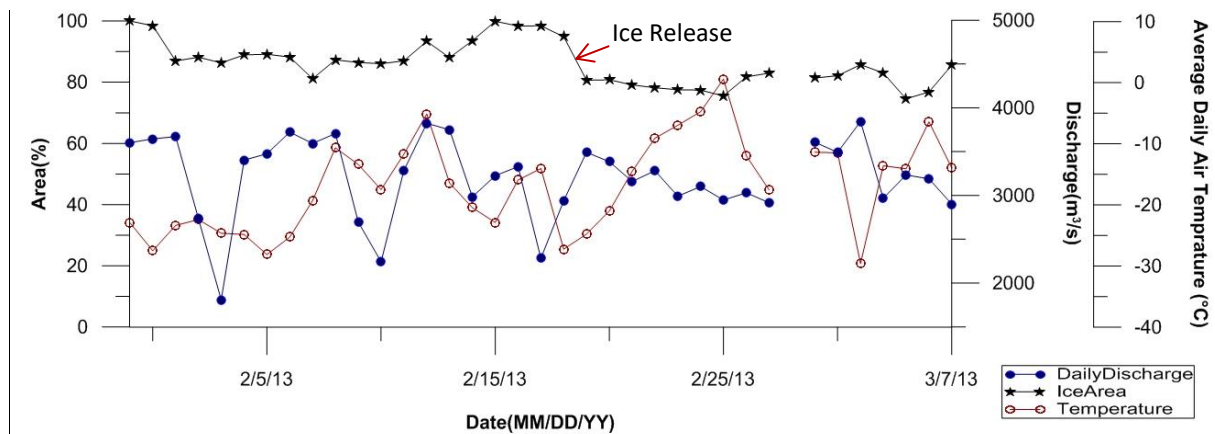


Figure 4: Extracted river ice cover area, water discharge and average daily air temperature at DX location along LNR for the period January 30, 2013 to March 7, 2013

Thermal growth of river ice cover led to the production of smooth ice with different texture detectable by the automated image analysis algorithm (Figure 3-b). Thermal ice periodically was produced in the open water area and it was advected out of camera field of view after its detachment from the ice cover body. A major detachment of the river ice cover within the open water patch is shown in Figure 4.

In order to estimate the volume of thermal ice production in the open water patch from the observed ice area, ice thickness was calculated using Stefan's ice cover growth equation. This method uses the cumulative Freezing Degree Days in degrees Celsius (FDD) to calculate the thermal ice cover thickness. In Stefan's equation as presented below (Stefan,1889),  $\alpha$  is an empirical coefficient depending on the site,  $k_i$  is the thermal conductivity of river ice ( $2.24 \text{ W m}^{-1} \text{ }^\circ\text{C}^{-1}$ ),  $\rho_i$  is the density of ice ( $916 \text{ kg m}^{-3}$ ) and  $\lambda$  is the latent heat of freezing ( $3.34 \times 10^5 \text{ J kg}^{-1}$ ) of ice.

$$[1] h_i = \alpha \sqrt{\frac{2k_i}{\rho_i \lambda} FDD}$$

This formula has been used in several other studies to estimate and simulate thermal river ice cover growth. Stefan's formula can be simplified to the following equation, in this case  $\beta$  is site dependent and based on Michel 1971 it varies between  $1.3 \sim 1.7 \text{ (}^\circ\text{C}^{-1/2} \cdot \text{Day}^{-1/2}\text{)}$ .

$$[2] h_i = \beta \sqrt{FDD}$$

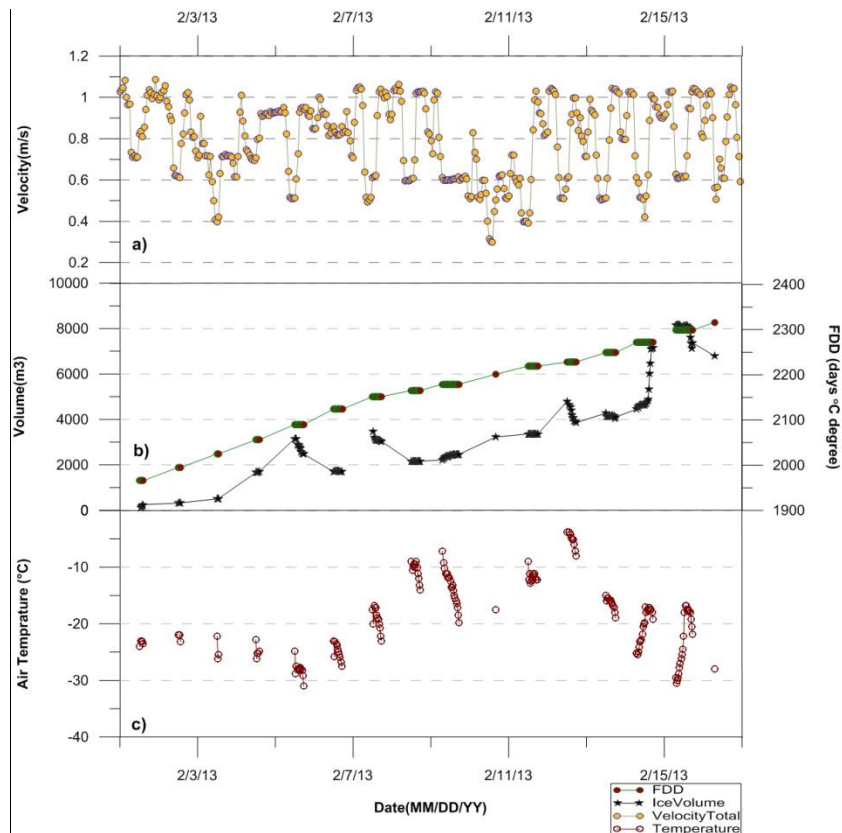


Figure 5: a) Average water velocity at DX location b) Extracted thermal ice volume production in an open water patch, and Freezing Degree Days (FDD) c) air temperature at DX location along LNR (February 2013)

Figure 5 shows for the DX location the hourly distribution of Freezing Degree Days (FDD), generated thermal ice and section averaged water velocity (discharge divided by section area). The developed image analysis algorithm was used to detect the thermal river ice cover and calculate its area, while the thickness of the generated river ice cover was calculated using Stefan's formula. These results were used to estimate the thermal river ice cover volume. The hourly results show that more important than air temperature, the increase in water velocity led to thermal ice cover deterioration due to detachment of thermal ice from borders of the open water patch.

#### 4.4 Jackfish Island:

The relatively mild slope of the river at this location allowed a comprehensive study for three winters (2012 to 2015). The total monitoring area at this location was around 492408 m<sup>2</sup>. While border ice growth and open water patch were monitored in the first two years, in the last winter ice break up was the primary goal of the research. Detailed results of this study are presented in (Ansari et al. in revision). In this section extracted results of the border ice growth at the Jackfish Island location are explained. Figure 6 shows a view of Jackfish Island with the formed border ice. Terrestrial monitoring at this location started in the second week of November 2013 and continued until March 2014. Figure 7 shows the average air temperature along with the area percentage covered by river ice and water surface. As is shown in this figure the algorithm was able to calculate and quantify the amount of river ice cover as river ice floes and border ice formed at the front edges of Jackfish Island (Figure 7). In Figure 8 it is demonstrated that the border ice cover increase at the shores of the island has a direct relation with temperature drop and increase in freezing degree days, although comprehensive statistical investigation is needed to verify this relation.

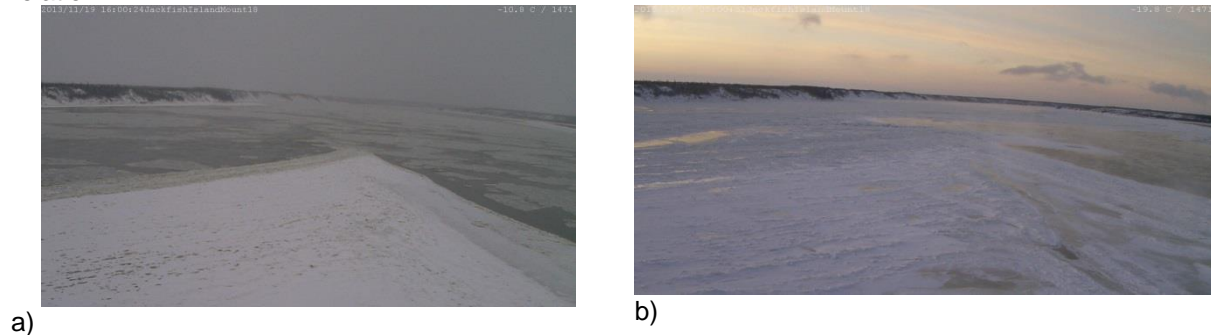


Figure 6: Jackfish Island site. a) taken on November 2013, b) taken on January 2014

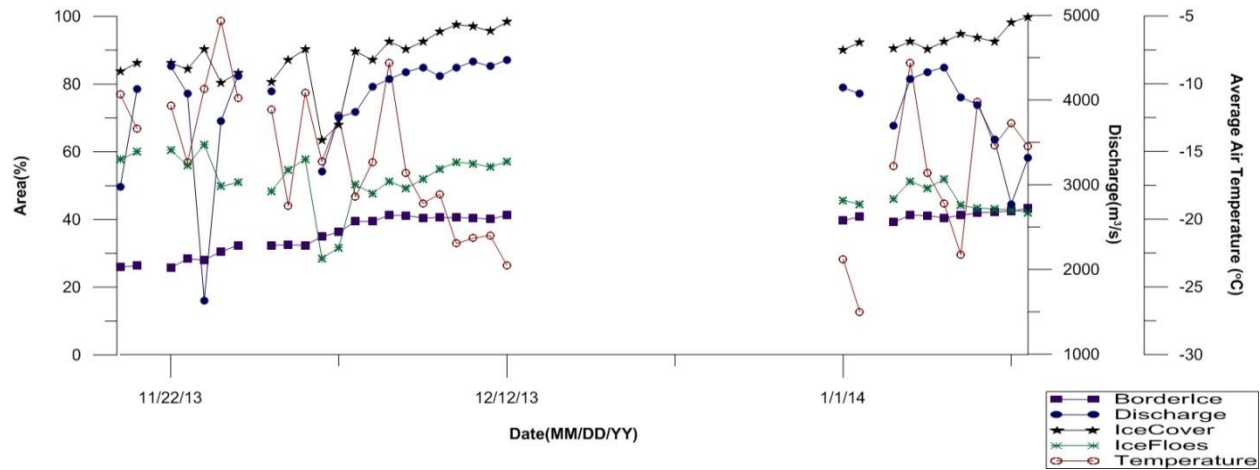


Figure 7: Water discharge, river ice cover area and air temperature quantified extracted results from time series of the Jackfish Island images (Duration of November 2013 to February 2014)



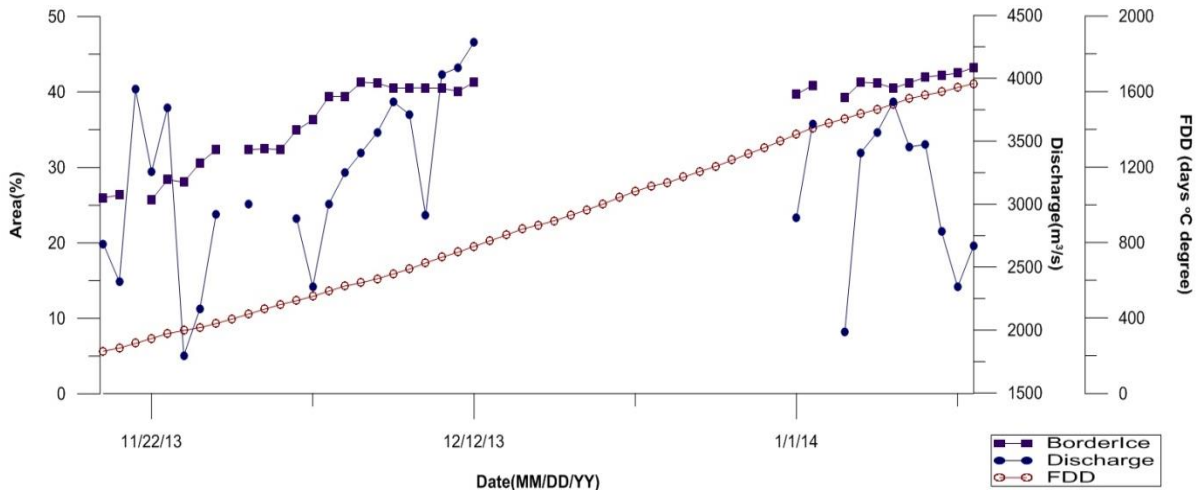


Figure 8: Water discharge, border ice growth at leading edge of the Jackfish Island and freezing degree days at this location (Duration of November 2013 to February 2014)

## 5 Conclusions:

An automated image analysis algorithm was developed to extract quantified data from the time series images of the shore-based terrestrial monitoring. This algorithm consists of five subroutines as: “preprocessing”, “image registration”, “image rectification”, “target detection” and “final calculations”. While the two steps of pre-processing and image registration are considered as the pre-processing steps of the image analysis algorithm, the image rectification subroutine is used to assign correct real world coordinates to the pixels of the images using the DEM map and camera intrinsic and extrinsic characteristics such as Field of View (FOV). Some modifications were added to this method to consider the water surface fluctuations in the river. For the “target detection” algorithm a categorization method was added to a variational thresholding technique developed by (Ray & Saha 2006). The categorization algorithm increased the applicability of the algorithm for detection of water and ice cover surfaces from time series images.

At DX location it was observed that the rate of thermal river ice production on the borders of an open water patch can be quantified using the developed algorithm. Periodical production and advection of the thermal ice cover in the open water patch shows the importance of water flow intensity in river ice cover formation. On the other hand, at Jackfish Island the ice floes and the border ice cover at the upstream island edge were monitored. It was shown that the border ice growth is mainly due to the decrease of air temperature. The leading edge of the thermal ice that is formed on the borders of this island grows until reaching to the other sections to form a stable ice cover across the river. The unique ability of the developed algorithm to extract quantified data from images demonstrates its suitability for automated analysis of shore-based terrestrial imagery.

## Acknowledgements

The authors would like to thank Nathan Lambkin and his crew from Manitoba Hydro for all their help and contributions during field measurements, including deployment and retrieval of instruments. This work was funded by Manitoba Hydro (R&D grant), Hatch corporation Ltd., and the Natural Sciences and Engineering Research Council of Canada (CRD grant).

## References

- Ansari, S., Rennie, C.D., Seidou, O., Malenchak, J., Zare, S.G., (In Revision) Automated Monitoring of River Ice Processes using Shore-based Imagery. *Cold Regions Science and Technology*.
- Corripio, J.G., Durand, Y., Guyomarc'h, G., Mérindol, L., Lecorps, D. and Pugliése, P., 2004. Land-based remote sensing of snow for the validation of a snow transport model. *Cold Regions Science and Technology*, 39(2-3), pp.93–104. <http://dx.doi.org/10.1016/j.coldregions.2004.03.007>
- Corripio, J.G., Javier G., 2004. Snow surface albedo estimation using terrestrial photography. *International Journal of Remote Sensing*, 25(24), pp.5705–5729. <http://dx.doi.org/10.1080/01431160410001709002>
- Ghareh Aghaji Zare, S., Asce, S.M., et al., 2016. Boundary Shear Stress in an Ice-Covered River during Breakup. *American Society of Civil Engineers*, 142(4), pp.1–14. DOI: 10.1061/(ASCE)HY.1943-7900.0001081
- Ghareh Aghaji Zare, S. Moore S., Rennie C.D., Seidou, O., Ahmari, H., 2014. Influence of river ice break-up on stream hydraulics and sediment transport. *River Flow 2014 – Schleiss et al. (Eds)*, pp.951–959.
- Goshtasby, Ardeshir, "Piecewise linear mapping functions for image registration" *Pattern Recognition*, Vol. 19, 1986, pp. 459-466. doi:10.1016/0031-3203(86)90044-0
- Goshtasby, Ardeshir, "Image registration by local approximation methods" *Image and Vision Computing*, Vol. 6, 1988, pp. 255-261. doi:10.1016/0262-8856(88)90016-9
- Guo, X., Yang, K., Fu, H., Xia, Q., Wang, T. and Yang, S., 2016. Ice processes modeling during reverse water transfer of open canals: a case study. *Journal of Hydro-environment Research*. <http://dx.doi.org/10.1016/j.jher.2016.03.002>
- Hough, P.V.C. Method and means for recognizing complex patterns, U.S. Patent 3,069,654, Dec. 18, 1962
- Härer, S. Bernhardt, M., Corripio, J. G., & Schulz, K., 2013. PRACTISE – Photo Rectification And ClassificaTion SoftwarE (V.1.0). *Geosci. Model Dev*, 6, pp.837–848. doi:10.5194/gmd-6-837-2013
- Jędrzychowski, K. & Kujawski, A., 2014. Method of image analysis in the process of assessment of ice occurrences. *Zeszyty Naukowe/Akademia Morska w Szczecinie*, 37(109), pp.45–49.
- Kaufmann, V., 2012. The evolution of rock glacier monitoring using terrestrial photogrammetry: The example of Ausseres hochebenka
- Ranjie, H.O.U. & Huimin, L.I., 1987. Modelling of BOD-DO dynamics in an ice-covered river in Northern China. *Pegman Journals Ltd*, 21(3), pp.247–251.
- Ray, N. & Saha, B.N., 2006. Edge sensitive variational image thresholding. *Proceedings - International Conference on Image Processing, ICIP*, 6. DOI: 10.1109/ICIP.2007.4379515
- Tang, G. et al., 2016. Modelling and Analysis of Hydrodynamics and Water Quality for Rivers in the Northern Cold Region of China. *International Journal of Environmental Research and Public Health*, 13(4), p.408. Available at: <http://www.mdpi.com/1660-4601/13/4/408>. doi:10.3390/ijerph13040408